N-terminal domains of fibrillin 1 and fibrillin 2 direct the formation of homodimers: a possible first step in microfibril assembly

Timothy M. TRASK, Timothy M. RITTY, Thomas BROEKELMANN, Clarina TISDALE and Robert P. MECHAM[1]

Department of Cell Biology and Physiology, Washington University School of Medicine, Box 8228, 660 South Euclid Avenue, St. Louis, MO 63110, U.S.A.

Aggregation of fibrillin molecules via disulphide bonds is postulated to be an early step in microfibril assembly. By expressing fragments of fibrillin 1 and fibrillin 2 in a mammalian expression system, we found that the N-terminal region of each protein directs the formation of homodimers and that disulphide bonds stabilize this interaction. A large fragment of fibrillin 1 containing much of the region downstream from the N-terminus remained as a monomer when expressed in the same cell system, indicating that this region of the protein lacks dimerization domains. This finding also confirms that the overexpression of fibrillin fragments does not in itself lead to spurious dimer formation. Pulse–chase analysis demonstrated that dimer formation occurred intracellularly, suggesting that the process of fibrillin aggregation is initiated early after biosynthesis of the molecules. These findings also implicate the N-terminal region of fibrillin 1 and fibrillin 2 in directing the formation of a dimer intermediate that aggregates to form the functional microfibril.

Key words: elastin, elastic fibres, extracellular matrix.

INTRODUCTION

The extracellular space contains an extensive array of matrix molecules that have important roles in influencing and directing tissue integrity, cell migration, cell shape, proliferation, secretion and differentiation. All extracellular matrices are deposited in a precise manner and have final structures and functions that are dependent on their tertiary structure, covalent and non-covalent interactions, and post-translational modifications of constituent macromolecules. The structural and functional integrity of the extracellular matrix is determined, in large part, by the ability of the cell to organize monomeric units into complex polymers. Much of the information for macromolecular assembly is contained within the matrix proteins themselves that can direct interactions between similar molecules (homotypic interactions) or between different molecules (heterotypic assembly).

We are interested in studying the assembly of microfibrils, a class of matrix molecule that forms fibrillar structures in the extracellular space. Microfibrils are 10–12 nm filaments first identified as components of elastic fibres, although they are also found in tissues devoid of elastin such as the ciliary zonules of the eye [1]. Rotary shadowing electron microscopy reveals microfibrils as linear arrays of electron-dense 'beads' separated by approx. 50 nm with filamentous 'strings' [2–4]. Although their function in the extracellular space has not been fully characterized, microfibrils are hypothesized to act as a molecular scaffold for the deposition and alignment of tropoelastin molecules [5,6]. This alignment permits the proper cross-linking and maturation of elastic matrices, such as those found in the lung and blood vessels. More recently it has been suggested that microfibrils have a role in the structural integrity and elasticity of tissues [7–9].

The major structural elements of microfibrils consist of an oligomer of fibrillin 1 (fib-1) and/or fibrillin 2 (fib-2) [10–12]. These approx. 350 kDa proteins are integral components of microfibrillar function, because mutations in each gene are linked to the human diseases Marfan syndrome (fib-1) and congenital contractural arachnodactyly (fib-2) [13–15]. Fib-1 and fib-2 have significant similarity to each other, both in primary sequence and predicted protein domains [12,16,17]. For example, each possesses tandem arrays of epidermal growth factor (EGF)-like domains and eight-Cys domains, the latter having been first described in latent TGF-β-binding protein 1 (LTBP-1) [18]. There is, however, one region of each protein that is distinctive: exon 10 of fib-1 encodes a Pro-rich region, whereas the analogous region in fib-2 contains a Gly-rich sequence.

It is unknown how the fibrillins interact or how many fibrillin molecules form the final microfibrillar structure. It is reasonable to assume that microfibril assembly occurs in several discrete steps. The early events of microfibril assembly are believed to involve the formation of fibrillin aggregates, potentially mediated by disulphide bonds [19–21]. This idea is supported by the finding that reducing agents are required to extract microfibrils from tissues [22]. In addition, immunoprecipitation studies showed a fraction of fib-1 molecules migrating at a size larger than a monomer under non-reducing conditions [19,21]. These high-molecular-mass species were thought to be dimeric [19], although the inability to resolve such large species by electrophoresis makes the determination of their true size difficult. It is also unknown whether this high-molecular-mass complex represents a homodimer of fib-1 or fib-1 complexed with fib-2 or some other protein. Later steps in microfibril assembly are even less well understood.

The work described here was undertaken to study early events of microfibril assembly by localizing the domains within fib-1 and fib-2 responsible for disulphide-bonded multimer formation. Accumulating evidence suggests that fibrillin molecules are stacked on one another in register within microfibrils, implying that interactions occur between analogous regions of neighbouring molecules [23]. We have focused on the Pro-rich domain of fib-1 and the Gly-rich domain of fib-2 because it is here that the molecules have the greatest difference in sequence. When the

Abbreviations used: CHO, Chinese hamster ovary; DTT, dithiothreitol; EGF, epidermal growth factor; fib, fibrillin; GMEM, Glasgow minimal essential medium; NEM, *N*-ethylmaleimide.

[1] To whom correspondence should be addressed (e-mail bmecham@cellbio.wustl.edu).

proteins are expressed in mammalian cells, we have found that a fib-2 fragment containing the Gly-rich region, downstream EGF-like domains and most of the second eight-Cys domain forms a disulphide-bonded homodimer. A similar propensity to form dimers was observed for the analogous region of fib-1, which contains the Pro-rich region and includes a completed second eight-Cys domain. Furthermore, we have determined that homodimer formation occurs only intracellularly. These results suggest that the early events of microfibril assembly might involve fibrillin homodimers, formed shortly after biosynthesis through parallel interactions near the monomer's N-terminus.

EXPERIMENTAL

Materials

All reagents were obtained from Sigma Chemical Co. (St. Louis, MO, U.S.A.) or Fisher Scientific (Pittsburgh, PA, U.S.A.) unless noted otherwise. Protein molecular mass standards and polyacrylamide gel reagents were from Bio-Rad Laboratories (Hercules, CA, U.S.A.). Restriction enzymes were purchased from Gibco–BRL (Gaithersburg, MD, U.S.A.) and Boehringer Mannheim (Indianapolis, IN, U.S.A.). All tissue culture media and supplements were obtained through the Washington University Tissue Culture Support Center. Fib-2 constructs were generously provided by Dr. Francesco Ramirez (Mt. Sinai School of Medicine, Brookdale Center for Molecular Biology, New York, NY, U.S.A.). CHOK1 cells (CHO being Chinese hamster ovary) were a kind gift from Dr. Erika Crouch (Washington University School of Medicine, Department of Pathology, St. Louis, MO, U.S.A.).

Fibrillin constructs

DNA sequencing

Plasmid DNA was prepared and sequenced essentially as described by Del Sal et al. [24]. One-third of the isolated DNA was used for sequencing with 10 ng of primer and reagents from United States Biochemical (Cleveland, OH, U.S.A.).

Fib-2 constructs: Aik and NLRe/6

Fib-2 cDNA constructs were essentially those reported in a previous study [12]. All of our fib-1 and fib-2 constructs (see Figure 1 and Table 1) except LEEC-P1 used the fib-2 leader sequence contained within the cDNA construct R2C11. This construct contained 201 bp of 5′ untranslated sequence and 137 bp of translated sequence (Met-1 to Gln-46). On sequencing, five extra base pairs (AAGCC) were found after bp +137 and before the *Eco*RI linker used for cDNA library construction. Fib-2 cDNA sequences are in the GenBank database (accession no. U03272); numbering refers to that sequence [12,25].

The Aik cDNA construct was subcloned into the *Eco*RI site of pBS.SK− and spanned bp +1274 to +2256 (Gly-425 to Phe-752) (see Figure 1 and Table 1). A *Bcl*I/*Eco*RV fragment of R2C11 in pBS.SK− was ligated into Aik/pBS.SK− cut with *Bam*HI/*Sma*I to provide a leader sequence for Aik. Sequence analysis confirmed the fusion of R2C11 with Aik as predicted. Owing to the extra sequences noted above for R2C11 and junctional vector sequences, the peptide Ser-Arg-Ile-Arg-Trp-Ala-Ala was inserted between Gln-46 and Gly-425.

The NLR3e/6 construct was completed in several steps and consists of fib-2 sequences without interruption from bp −144 to +3342 (Met-1 to Thr-1114) along with a C-terminal hexahistidine tag (see Figure 1 and Table 1). Reverse transcription and amplification were used to fill in a 10 nt gap in the available cDNA clones with total RNA obtained from MG63 cells (ATCC no. CRL-1427; American Tissue Type Collection, Rockville, MD, U.S.A.) with the use of the procedure described by Sambrook et al. [26]. Primers were designed to amplify bp −151 to +250. Nucleotide −139 was changed from dA to dC to create an *Nhe*I site in the 5′ primer, whereas nt +227, +228 and +232 were changed from dG to dA, from dG to dT and from dG to dT respectively to create a *Cla*I site in the 3′ primer. An *Eco*RI site was also added to the 3′ primer. The 400 bp amplified fragment was digested with *Nhe*I/*Eco*RI and ligated into the vector pNsCH that was cut with the same enzymes. pNsCH is a modified pBS.SK−, where (1) the *Hin*dIII site was cut, blunted with Klenow fragment of DNA polymerase I (Gibco-BRL), and religated to create an *Nhe*I site and (2) the *Cla*I site was destroyed by digestion with *Cla*I, blunting and religation. An *Msc*I/*Cla*I fragment of cDNA clone E/C (bp +209 to +1080), a *Cla*I/*Eco*RI fragment of cDNA clone Ao6 (bp +1075 to +1279) and an *Eco*RI/*Xba*I fragment from cDNA clone 13.25 (bp +2251 to +3320) were then added sequentially, followed by an *Eco*RI/*Eco*RI fragment of cDNA clone Aik (bp +1274 to +2256). Because the last seven residues of an EGF-like domain comprising bp +3321 to +3342 (Met-1108 to Thr-1114) were missing, overlapping and complementary oligonucleotides with overhanging *Eco*RI and *Hin*dIII sites were annealed together and ligated into the same sites in pBS.SK− containing a hexahistidine tag oriented with the 5′ side nearest to the *Hin*dIII site and where the endogenous *Xba*I site within the multiple cloning region was destroyed by digestion with *Xba*I, blunting and religation. An *Nhe*I/*Xba*I fragment of the construct described above was cloned into the *Xba*I site of EGF/p6His (contained within the introduced EGF primer), producing NLR3e/6. Sequencing was done for approx. 150 nt from both ends to verify 5′ sequences as well as the addition of the missing EGF-like domain residues and the hexahistidine tag at the 3′ end. The sequences of all junctions between the constructs were also verified as being correct. Base pair +3150 was read as dG, which was initially reported by Zhang et al. [12] as dA. However, there is no change in the amino acid (Thr-1050).

Fib-1 constructs: PET and LEEC-P1

The fib-1 construct PET (see Figure 1 and Table 1) was generated by reverse transcription and amplification by using total RNA obtained from MG63 cells as described above. PET spans bp +1168 to +2165 (Ser-390 to Ser-722; GenBank accession no. L13923 [17]). The 3′ primer was used for reverse transcription; 5′ and 3′ primers were used to amplify the cDNA. The product (1012 bp) was digested with *Xba*I and ligated into the *Xba*I site of pBS.SK−. DNA sequencing was done for approx. 200 bp from each end to verify its identity. A *Bcl*I–*Eco*RV fragment of R2C11/pBS.SK− (fib-2 leader sequence) was ligated to PET/pBS.SK− cut with *Bam*HI/*Spe*I (blunted). This junction was confirmed by DNA sequencing. Because of cloning constraints the peptide Ser-Arg-Ile-Arg-Ser-Ser-Ser-Arg occurred between R2C11 and PET and a valine residue at the C-terminus before the stop codon contained within the 3′ primer.

The cloning of construct LEEC-P1 and its expression in CHOK1 cells have been described [27]. LEEC-P1 possesses sequences from exon 1 containing the fib-1 leader sequence (Met-1 to Val-58) fused with exons 23–44 (Asp-910 to Asn-1848) and exons 64–65 (Ser-2688 to His-2871) (Figure 1 and Table 1). Arg-2731 was mutated to serine to prevent endoproteolytic processing of the C-terminus [27,28]. During cloning, the amino acids Arg and Thr were inserted between Val-58 and Asp-910; similarly the

peptide Ser-Gly-Ala-Ser was inserted between Asn-1848 and Ser-2688.

Expression of fibrillin constructs

All constructs were cloned into the pEE14 mammalian expression vector [29] with expression driven from the cytomegalovirus promoter/enhancer elements. NLR3e/6, LEEC-P1 and PET possessed their own stop codons, whereas Aik used a stop codon from downstream pEE14 sequences; consequently the peptide Asp-Ile-Lys-Leu-Ile-His was C-terminal to Phe-752. Cloning sites for the constructs were as follows: PET, *Hin*dIII/*Xba*I fragment into the same sites in pEE14; Aik, *Xba*I/*Hin*dIII (blunted) fragment into the *Xba*I/*Eco*RI (blunted) sites in pEE14; NLR3e/6, *Nhe*I/*Spe*I fragment into the *Xba*I site in pEE14. Constructs were checked for proper orientation; DNA was purified for transfection (Qiagen, Chatsworth, CA, U.S.A.).

CHOK1 cells were transfected essentially as described by Crouch et al. [30]. Cells were plated at $(2–4) \times 10^5$ cells per 60 mm dish (Fisher Scientific) in Glasgow minimal essential medium (GMEM)-10 containing 2 mM L-glutamine [29]. The following day, the CHOK1 cells were washed twice with glutamine-containing GMEM and transfected with 9 μg of DNA/30 μl of Lipofectin for Aik and NLR3e/6 or with 9 μg of DNA/20 μl of Lipofectamine for PET (Gibco–BRL). Cells were transfected for 6–24 h, after which glutamine-containing GMEM-10 was fed to the cells. On the second day after transfection, cells were split 1:3 into 100 mm dishes and maintained in GMEM-10 containing 25 μM L-methionine sulphoximine. Cells were refed twice per week with this selection medium. Colonies were isolated with the use of cloning rings and assayed for expression of the constructs. Aik/CHO, PET/CHO and NLR3e/6-CHO cells were further subcloned by using single-cell dilutional cloning.

Antibodies

cDNA constructs for Aik (see above) and a clone encoding the Pro-rich region of fib-1 (Ser-390 to Asn-448) prepared by PCR of RNA obtained from MG63 cells were inserted into the pQE vector (Qiagen), which contains an N-terminal hexahistidine tag. Polyclonal antibodies were made in rabbits against bacterially expressed proteins, which were purified over a Ni^{2+}/NTA–agarose column (Qiagen) equilibrated in 6 M guanidine/50 mM sodium phosphate (pH 8.0) and eluted with the same buffer at pH 5.0. All antisera were enriched for IgG by performing a precipitation with octanoic acid [31].

Western blot analysis

Serum-free GMEM-10 medium (containing 2 mM L-glutamine) from 24–48 h incubations with transfected cells was centrifuged to remove cell debris; aliquots were subjected to SDS/PAGE. Reduced samples contained 50 mM dithiothreitol (DTT). After electrophoresis, gels were soaked in 10 mM 3-[cyclohexylamino] propane-1-sulphonic acid (pH 11.0)/10 % (v/v) methanol for 10 min. Proteins were transferred to nitrocellulose for 1 h in the same buffer at 60–70 V. Nitrocellulose blots were blocked in 3 % (w/v) non-fat milk in PBS and developed as described [27].

Pulse–chase analysis and immunoprecipitation

Cells were labelled with 40 μCi/ml [^{35}S]cysteine (ICN, Costa Mesa, CA, U.S.A.) for 5 h in serum-free Dulbecco's modified Eagle's medium lacking L-cysteine, supplemented with 1 mM sodium pyruvate and non-essential amino acids (each at 100 μM). Medium was collected and centrifuged to pellet any detached cells. The cell layer was washed three times in PBS and then lysed for 10 min at room temperature in 50 mM Tris/150 mM NaCl/0.5 % deoxycholate/1 % (v/v) Triton X-100/0.1 % SDS/2.5 mM EDTA/0.1 mM PMSF (pH approx. 7.0) (IP buffer). For some experiments, cells were lysed in the dark with IP buffer containing the alkylating agents 1 mm iodoacetamide and 1 mM *N*-ethylmaleimide (NEM). For pulse–chase experiments, cells were pulsed with [^{35}S]cysteine for 5 min and then chased for various durations in HyQ-CCM5 (Hyclone Laboratories, Logan, UT, U.S.A.) medium without radiolabel after two washes. At each time point, the medium was collected and the cells were immediately lysed in IP buffer containing 0.2 mM ϵ-aminohexanoic acid and 0.5 mM benzamidine for 2 min at room temperature. Cells were washed three times with PBS before lysis for the 30 and 60 min time points. Cellular material and associated extracellular matrix were scraped from the dish and the lysate was spun at 16000 ***g*** to pellet insoluble material.

For immunoprecipitation, the medium and soluble cell lysate were incubated with Protein A/Trysacryl beads (Pierce Chemical, Rockford, IL, U.S.A.)/100 μg/ml BSA (Fraction V)/25–50 μg/ml polyclonal antibodies at 4 °C overnight. The beads were then washed four times with PBS/0.5 % (v/v) Tween 20, and bound material was eluted in SDS/PAGE sample buffer [62.5 mM Tris/HCl (pH 6.8)/0.4 % SDS/10 % (v/v) glycerol/0.003 % Bromophenol Blue]. Reduced samples contained 50 mM DTT. Samples were subjected to SDS/PAGE, fixed with 40 % (v/v) methanol/7 % (v/v) acetic acid, incubated with 15 % (v/v) methanol/1 M salicylic acid, then subjected to autoradiography.

Assessment of extracellular disulphide bond formation

Transfected cells were radiolabelled for 5 h. The media were collected, centrifuged to pellet cells, then diluted 1:1 with supplemented Dulbecco's modified Eagle's medium containing 10 % (v/v) fetal bovine serum (Hyclone Laboratories). Aliquots were either placed in tubes at 37 °C in a CO_2 incubator or added to confluent untransfected CHOK1 cells. At various times, aliquots were collected and subjected to immunoprecipitation. BSA was omitted from the immunoprecipitation because serum was included in the incubations.

Purification of Aik and amino acid analysis

Aik was concentrated from conditioned medium by 50 % (w/v) $(NH_4)_2SO_4$ precipitation. The precipitate was pelleted and then resuspended in PBS containing 0.05 % (v/v) trifluoroacetic acid. This material was applied to a C_4 reverse-phase HPLC column (10 mm × 250 mm; Vydac, Hesperia, CA, U.S.A.) and eluted with a linear gradient of 20–70 % (v/v) acetonitrile/0.05 % (v/v) trifluoroacetic acid at a flow rate of 150 ml/h. Aik was more than 90 % pure in fraction 15 on the basis of Coomassie-stained gels. Aik monomer and dimer in this fraction were separated by using a S6 Superose sizing column (10 mm × 300 mm; Pharmacia Biotech, Piscataway, NJ, U.S.A.) at a flow rate of 30 ml/h, equilibrated in 0.5 × PBS. Fractions were dried and then hydrolysed overnight at 110 °C in constant-boiling HCl. The amino acid composition was determined with a Beckman System 6300 amino acid analyser.

RESULTS

Expression of fib-1 and fib-2 constructs in CHOK1 cells

For this study, constructs containing the N-terminal regions of fib-1 and fib-2 as well as a central region of fib-1 were expressed

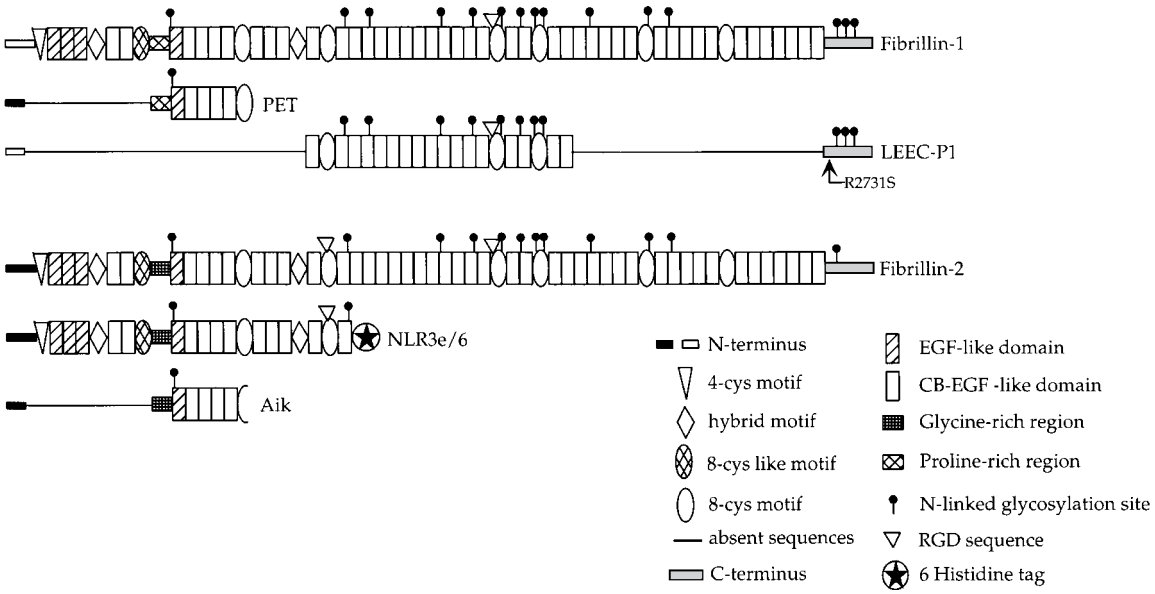

Figure 1 Schematic diagram of the fib-1 and fib-2 constructs expressed in CHOK1 cells

Symbols indicate the motifs present in the fibrillins [12,16,17]. The thin line connecting the domains represents absent sequences. Abbreviation: CB-EGF-like domain, Ca^{2+}-binding EGF-like domain.

Table 1 Details of the constructs shown schematically in Figure 1

Constructs Aik, NLR3e/6 and PET contained the leader sequence from fib-2; LEEC-P1 used the fib-1 leader sequence. In Aik the second 8-Cys domain was incomplete, with only seven Cys residues. The molecular masses shown do not take cleavage of the leader sequence into account.

Construct (fib)	Amino acid residues (fib)	Molecular mass (kDa)
Aik (2)	Met-1 to Gln-46 (2), Gly-425 to Phe-752 (2)	40.7
NLR3e/6 (2)	Met-1 to Thr-1114 (2)	120.3
PET (1)	Met-1 to Gln-46 (2), Ser-390 to Ser-722 (1)	42.5
LEEC-P1 (1)	Met-1 to Val-58 (1), Asp-910 to Asn-1818 (1), Ser-2600 to His-2871 (1)	129.9

in CHOK1 cells, depicted schematically in Figure 1 and Table 1. The fib-2 construct, Aik, begins five residues into the Gly-rich region [12] and extends into the second eight-Cys domain, ending three residues short of the eighth cysteine; therefore Aik has only seven cysteine residues. NLR3e/6 contains continuous sequences from the initiator methionine of fib-2 to the first EGF-like domain after the third eight-Cys domain and therefore encompasses the region represented by Aik. PET includes the first residue of the Pro-rich domain of fib-1 [17] and ends with the last residue predicted for the second eight-Cys domain. LEEC-P1 contains the leader sequence of fib-1 spliced to the large central region of EGF-like domains (exons 23–44) and the C-terminal domain (exons 64–65) of fib-1. Figure 2 demonstrates that these proteins were stably expressed in CHOK1 cells as assessed by immunoprecipitation or Western blotting. All constructs, especially LEEC-P1, migrated on SDS/PAGE gels at sizes larger than predicted. Digestion with peptide N-glycosidase or treatment of the cells with tunicamycin confirmed that all constructs were N-linked glycosylated, as predicted by their primary sequences (results not shown).

N-terminal fragments of fib-2 (Aik, NLR3e/6) and fib-1 (PET) form disulphide-bonded dimers

A Western blot for Aik from conditioned medium under non-reducing conditions showed two bands, one migrating at a size predicted for a dimer and the other at a size predicted for a monomer (Figure 3). These bands were also seen when Aik was immunoprecipitated from either medium or cell lysate (Figure 3). As predicted for a disulphide-bonded interaction, reduction with DTT caused the dimeric species to shift to monomeric size. The electrophoretic mobility of the reduced monomer was also slightly decreased relative to unreduced monomer, presumably owing to the altered conformation of the protein on reduction of the EGF-like domains. Interestingly, immunoreactive bands were seen in the medium of Aik/CHO cells at approx. 200 kDa that were not seen in untransfected CHOK1 cells, perhaps indicating the higher-order multimerization of Aik (Figure 3). This multimerization seemed to be mediated by disulphide bonds because reduction caused its disappearance from this size range.

It has been shown that all eight cysteine residues in the fourth

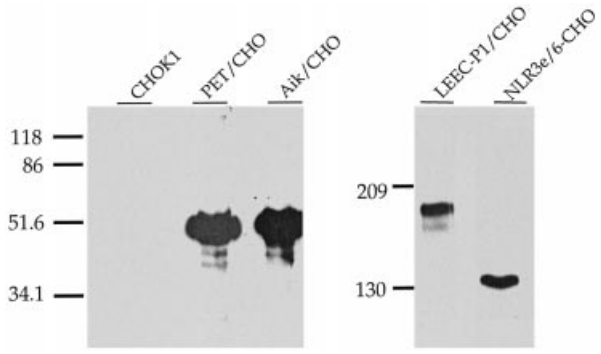

Figure 2 Expression of the fib-1 and fib-2 constructs in CHOK1 cells

For Aik and PET, a Western blot was done on reduced conditioned medium from untransfected CHOK1 cells and CHOK1 cells expressing each of the constructs. For NLR3e/6 and LEEC-P1, an immunoprecipitation was performed on conditioned medium from transfected cells labelled with [^{35}S]cysteine; immunoprecipitates were run under reducing conditions. The anti-Aik polyclonal antibody was used to detect Aik and NLR3e/6, whereas the anti-Pro antibody was used to detect PET. LEEC-P1 was immunoprecipitated with a polyclonal antibody directed against exons 64–65 of fib-1. The positions of molecular mass markers are indicated (in kDa) at the left of each panel.

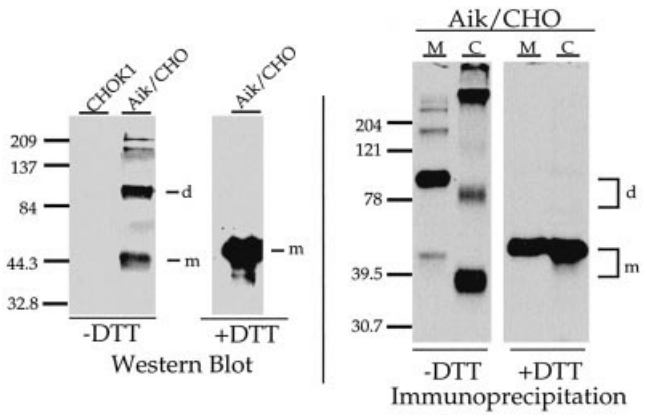

Figure 3 Aik demonstrates monomeric- and dimeric-sized bands under non-reducing conditions

Left panel: Western blot for Aik from conditioned medium with the use of anti-Aik antibody. Right panel: immunoprecipitations for Aik from medium and cell lysate by using anti-Aik antibody were subjected to electrophoresis under reducing (+DTT) and non-reducing (—DTT) conditions. Abbreviations: d, dimer; m, monomer; M, medium; C, cell layer.

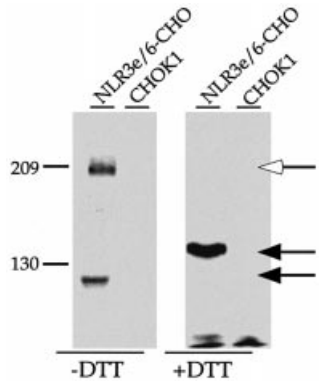

Figure 4 NLR3e/6 forms disulphide-bonded dimers

An immunoprecipitation for NLR3e/6 run under reducing (+DTT) and non-reducing (—DTT) conditions from the cell lysate is shown with the use of anti-Aik antibody. The cells were lysed in the presence of alkylating agents. The open arrow indicates the dimer; the filled arrows indicate the monomer.

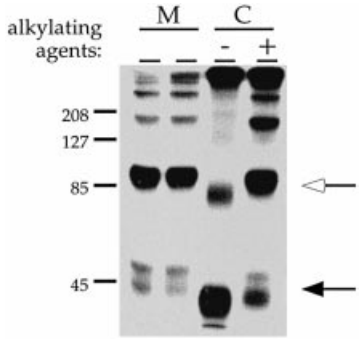

Figure 5 Aik forms dimers in the presence of alkylating agents

Immunoprecipitation for Aik from the cell layer with the use of anti-Aik antibody after cells were lysed in the presence of 1 mM NEM and 1 mM iodoacetamide shows an enhanced formation of dimers over untreated lysate. The medium was untreated and served as a positive control for the expression of Aik. The open arrow indicates the dimer; the filled arrow indicates the monomer. Abbreviations: M, medium; C, cell layer.

eight-Cys domain of fib-1 might be involved in intramolecular disulphide bonds [23]. Therefore it was possible that Aik dimer formation occurred through non-specific intermolecular disulphide bonding via the unpaired cysteine residue in the second eight-Cys domain. This seems unlikely, however, because the expression of Aik constructs containing a filled-in eight-Cys domain (results not shown) as well as NLR3e/6, a construct that encompasses a large portion of the N-terminal region of fib-2, including the region represented by Aik, formed disulphide-bonded dimers in the cell lysate (Figure 4). Furthermore, even when the Aik/CHO cells were lysed in buffers containing the thiol-alkylating agents iodoacetamide and NEM, dimers of Aik were evident (Figure 5). In fact, there seemed to be enhanced stabilization of the dimer in the cell lysate under these conditions (compare Figure 5, lanes 3 and 4). Additionally, the size difference between monomers and dimers in the medium compared with the cell lysate also disappeared, perhaps indicating that in the absence of alkylating agents Aik undergoes some type of conformational change.

To characterize the constituents of the dimeric band, the monomer and dimer of Aik were purified with a C_4 reverse-phase HPLC column. Coomassie staining showed co-elution of monomer, dimer and multimers purified to more than 90% by this method (Figure 6a). Western blotting confirmed that these bands contained Aik (results not shown). The monomer and dimer were then separated with a Superose 6 sizing column (Figure 6b). Figures 6(c) and 6(d) demonstrate that this approach effectively separated monomer from dimer, as assessed by both Coomassie staining and Western blotting. Higher-order multimers of Aik were also co-eluted with the dimer. Fractions enriched in monomer or dimer were subjected to amino acid analysis and were found to have identical compositions, consistent with values predicted for Aik from its cDNA sequence (results not shown). These findings indicate that the dimeric band was a homodimer of Aik and not Aik complexed with a CHOK1-derived protein.

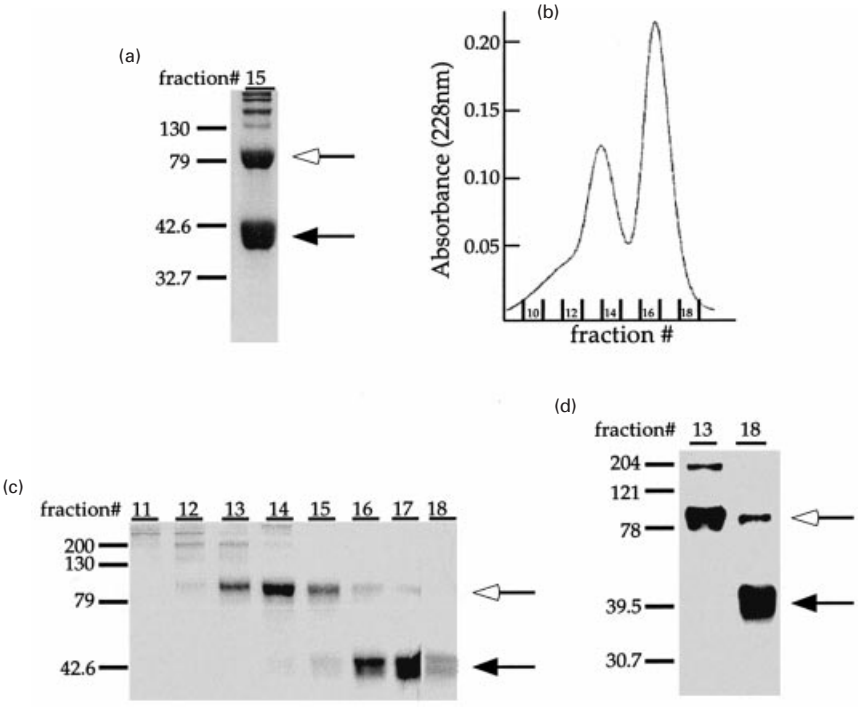

Figure 6 Purification and physical separation of Aik monomer and dimer

(**a**) Aik/CHO conditioned medium was concentrated and then applied to a C_4 reverse-phase HPLC column. Shown is a Coomassie-stained gel of fraction 15, which contained Aik monomer and dimer. (**b**) Separation of monomer and dimer from HPLC fraction 15 after application to a Superose 6 (S6) size column. The chromatogram from the column run is shown with corresponding fraction numbers. (**c**) Coomassie stain of the S6 fractions containing Aik monomer and dimer. Fraction 18 was run on a separate SDS/PAGE gel. (**d**) Western blot with the use of anti-Aik antibody on S6 fractions 13 and 18 to demonstrate the extent of separation; these were used for amino acid analysis. The open arrows indicate the dimer; the filled arrows indicate the monomer.

To determine whether the corresponding region of fib-1 might also direct dimer formation, immunoprecipitates of PET from medium and cell lysate were examined under reducing and non-reducing conditions. Figure 7 shows that PET migrated at sizes predicted for a monomer and dimer. As with Aik, reduction caused a shift of the PET dimer to monomeric size. This reduction-sensitive change in molecular mass was also observed with a baculoviral system for PET expression (results not shown). Immunoprecipitation of PET in the presence of alkylating agents had no demonstrable effect on the ratio of dimer to monomer in the cell lysate (results not shown). By analogy with Aik, we believe that PET was forming homodimers.

It is important to note that dimers not stabilized by disulphide bonds will dissociate to monomers on the SDS/gel system, leading to an underestimation of dimers. Therefore a possible explanation for variability in the dimer-to-monomer ratio observed for the various constructs used in this study might be a slower rate of dimer stabilization through disulphide exchange.

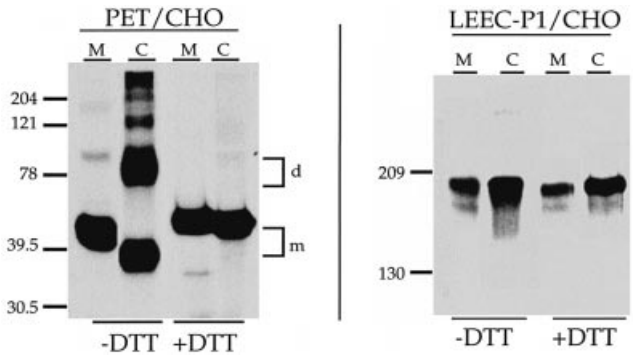

Figure 7 PET, but not LEEC-P1, forms dimers under non-reducing conditions

Immunoprecipitations for PET (left panel) and LEEC-P1 (right panel) from medium (M) and cell lysate (C) were subjected to electrophoresis under reducing (+DTT) and non-reducing (−DTT) conditions. Immunoprecipitations were performed with anti-Pro antibody (for PET) or an antibody directed against exons 64–65 of fib-1 (for LEEC-P1). Abbreviations: d, dimer; m, monomer.

Dimer formation does not occur with a fragment of fib-1 lacking the N-terminal region

To determine whether dimer formation was specific for the N-terminal region of the fibrillins or was a general property of any fragment of the molecules, we assessed whether a clone containing the central region and C-terminal domain of fib-1 (LEEC-P1) formed homodimers when expressed in CHOK1 cells. Like the N-terminal constructs, LEEC-P1 contained multiple EGF-like domains and eight-Cys domains but lacked the Pro-rich region. An immunoprecipitation for LEEC-P1 from medium and cell lysate (in the presence of alkylating agents) clearly showed the molecule to be monomeric in size with a minimal change in molecular mass after reduction (Figure 7). These results demonstrate that disulphide bond formation with PET, Aik and NLR3e/6 was not due to an artifact of overexpression of fibrillin fragments in CHOK1 cells rich in EGF-like and eight-Cys domains or a result of experimental manipulation.

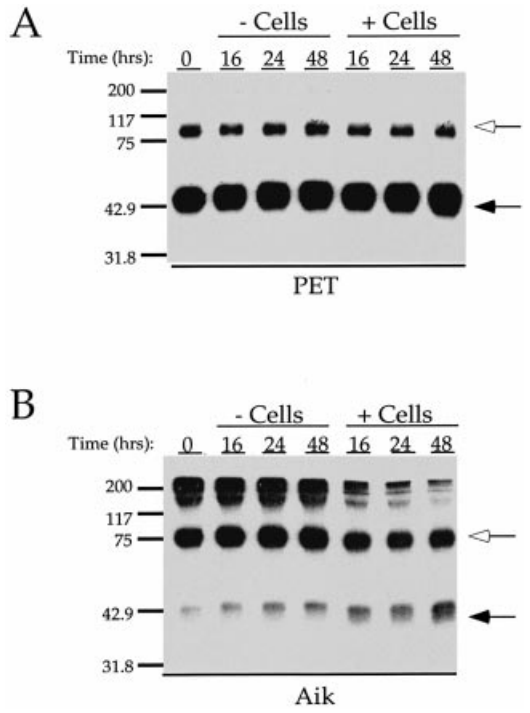

Figure 8 Aik and PET do not form dimers extracellularly after secretion from the cell

Radiolabelled conditioned media containing PET (**A**) or Aik (**B**) were either left in tubes (−cells) or incubated with untransfected CHOK1 cells (+cells) for the indicated durations before immunoprecipitation from the medium with anti-Pro antibody (for PET) or anti-Aik antibody (for Aik). The open arrows indicate the dimer; the closed arrows indicate the monomer.

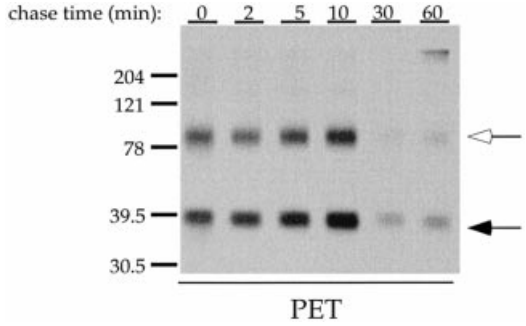

Figure 9 PET quickly dimerizes intracellularly after biosynthesis

PET/CHO cells were pulsed for 5 min with [^{35}S]cysteine and then chased for the indicated durations in unlabelled medium before cell lysis. Immunoprecipitations were performed with anti-Pro antibody from the cell lysate. The open arrow indicates the dimer; the closed arrow indicates the monomer.

Disulphide-bonded dimers form intracellularly

Covalent dimer formation did not form extracellularly, because monomer could not be chased into dimer after secretion into the medium. Incubating radiolabelled conditioned medium containing either Aik or PET with untransfected CHOK1 cells did not result in a conversion of monomer into dimer (Figures 8A and 8B). Identical results were obtained when the radiolabelled medium was incubated at 37 °C in the absence of cells. These findings also demonstrated the stability of the monomeric and dimeric forms of the molecules and provided further evidence that the dimer did not form during sample handling and preparation.

Intracellular formation of PET dimers was investigated by pulse–chase analysis with [^{35}S]cysteine with the use of short pulse times. In these experiments, dimers of PET could be immunoprecipitated from cell lysates immediately after the initial pulse of 5 min (Figure 9). The detection of dimers after this short labelling period confirmed their formation intracellularly, especially when considering a transit time of approx. 30–60 min for secretion of PET (results not shown).

DISCUSSION

Members of the fibrillin gene family serve as integral, core components of 10–12 nm microfibrils. Given the high cysteine content of fibrillin, it is not surprising that intermolecular disulphide bonds are important in stabilizing their macromolecular assembly [19–21]. Several studies have shown that high-molecular-mass aggregates, in addition to monomeric species, are observed after electrophoresis of fib-1 immunoprecipitates under non-reducing conditions [19,21]. It is unknown, however, whether the higher molecular mass aggregates are homopolymers or heteropolymers of fib-1 and fib-2. Recent evidence also demonstrates that transglutaminase-derived cross-links are involved in stabilizing fibrillin multimers [32]. These cross-links might explain the earlier observations that not all of the high-molecular-mass fibrillin aggregates are susceptible to reduction.

In studying the properties of N-terminal constructs of fib-1 and fib-2, we observed a propensity of these protein products for forming disulphide-bonded dimers under non-reducing conditions. Dimer formation was not unique to CHOK1 cells because reduction-sensitive changes in molecular mass were also seen when these constructs were expressed in Sf9 cells by using a baculoviral vector (results not shown). We do not believe that the presence of both monomer and dimer reflects an artifact of our expression system, as cells that normally express fib-1 and fib-2 also display both monomeric and dimeric forms of the full-length protein [19,21]. Furthermore, LEEC-P1 did not form dimers when expressed in CHOK1 (Figure 7, right panel) or Sf9 cells, indicating that this region of the protein lacks dimerization domains and that overexpression of fibrillin fragments does not in itself lead to spurious dimer formation. These findings with LEEC-P1 argue strongly that the ability to form disulphide-bonded dimers is specific to the regions in the fibrillins represented by PET and Aik. Preliminary results also demonstrate that heterodimers between these regions of the fibrillins do not occur, suggesting that the Pro-rich and Gly-rich domains of fib-1 and fib-2 respectively are important in determining the specificity of dimer formation.

It is intriguing that, for PET [and NLR3e/6 (results not shown)], more monomer than dimer was found in the medium, in contrast with that found intracellularly, where an approx. 1:1 ratio of dimer to monomer was consistently observed. At present we do not understand the disparity in the amount of dimeric PET between medium and cell lysate. We cannot exclude the possibility of selective degradation of PET dimer even though the ratio of monomer to dimer remained fairly constant during biosynthesis and transport through the cell (Figure 9) as well as after secretion (Figure 8).

Dimer formation occurs only intracellularly and not after secretion from the cell. As early as PET can be detected in cell

lysates, a significant amount of protein is in the form of disulphide-bonded dimer, suggesting that homodimer formation occurs early during biosynthesis in the endoplasmic reticulum. Interestingly, a difference in size between intracellular and secreted forms of the proteins was observed after radiolabeling (Figure 7, left panel). This difference in size is lessened somewhat by the inclusion of alkylating agents in the lysis buffer (results not shown). The remaining discrepancy in size can be explained by the observation that this construct is O-linked glycosylated (results not shown), a modification that occurs later in the secretory pathway.

The cysteine residues most likely to participate in dimer formation are those in the second eight-Cys domain of these constructs because there have been no reports of covalent linkage of cysteine residues between neighbouring EGF-like domains. It is assumed that all cysteine residues are disulphide bonded within the eight-Cys domain, because Reinhardt et al. [23] found that the cysteine residues in the fourth eight-Cys domain of fib-1 could not be chemically modified unless they were first reduced. However, the possibility that cysteine residues might be buried within the domain in the thiol form and thus inaccessible to chemical modification cannot be excluded. The eighth cysteine residue is not involved in dimer formation because Aik, which lacks the eighth cysteine residue, forms homodimers. It also seems that disulphide bond formation is specific to the second eight-Cys domain of fib-1 and fib-2 because LEEC-P1 contains three different eight-Cys domains yet does not dimerize. A precedent supporting disulphide rearrangement in eight-Cys domains is provided by Saharinen et al. [32], who found that rearrangement of cysteine residues in the third eight-Cys repeat of latent TGF-β-binding protein 1 (LTBP-1) is responsible for its covalent interaction with latent TGF-β.

We cannot discount the possibility that common N-terminal sequences from the fib-2 leader sequence (used for NLR3e/6, Aik and PET) are responsible for some step in homodimer formation. However, the ability to form disulphide-bonded dimers must lie outside this region, because the amino acids remaining after leader sequence cleavage in fib-2 are not predicted to contain cysteine residues [12].

Model for the assembly of fibrillin into microfibrils

Two models have been proposed to explain the organization of fib-1 within microfibrils. In both models, fibrillin molecules are linearly arranged in a head-to-tail manner; however, there is disagreement as to whether fibrillins are stacked on one another in the cross-sectional axis in register or in a staggered arrangement.

On the basis of immunohistochemical evidence, Reinhardt et al. [23] hypothesized that the stacked fibrillin molecules are in register and span from one beaded element to the next, with the N-terminus of one molecule and the C-terminus of the next close to or within the bead. There must be considerable packing of fibrillin to fit within this 50 nm space, which Reinhardt et al. believed to occur within the central region of uninterrupted EGF-like repeats. In the second model, a staggered arrangement was proposed by Qian and Glanville [33], who found that transglutaminase-derived cross-links join the N-terminal region of one fib-1 molecule with the C-terminal region of another. This linkage could form only if fib-1 molecules were in a staggered arrangement. Downing et al. [34] determined the NMR structure of an adjacent pair of EFG-like domains from fib-1 and found an extended conformation with a diameter of 2 nm. They concluded that EGF-like loops in fib-1 are unlikely to undergo the higher-order packing that would be required of the central region of EGF-like loops in the model postulated by Reinhardt et al. A staggered model supports the results of Qian et al. and Downing et al. whereby each fib-1 monomer spans two inter-bead regions. The propensity of our constructs to form disulphide-bonded homodimers is consistent with the parallel model of Reinhardt et al. To accommodate the cross-linking data obtained by Qian and Glanville, however, it is possible that disulphide-bonded fibrillin dimers, organized in register, accumulate within the microfibril in a staggered arrangement relative to other dimers.

We propose that the process of homodimer formation might be the initial event in microfibril assembly, with homodimers aggregating into polymers to form the functional fibre. A similar multistep process has been proposed for the assembly of tenascin into the six-subunit hexabrachion. In this case, sequences near the N-terminus of tenascin direct the formation of trimer intermediates. Subsequently, a second domain is responsible for the association of two triplets into a hexamer [35]. We suggest a similar process for the fibrillins, with homodimeric fibrillin, forming through interactions at the N-terminus, possibly being the molecular form that incorporates into the fibre. Presumably, interactions taking place within other regions of the fibrillins, not represented by our constructs, will complete the 'beads on a string' morphology.

This work was supported by grants HL53325, HL29594 and HL41926 to R. P. M.

REFERENCES

1 Cleary, E. and Gibson, M. (1983) Int. Rev. Connect. Tiss. Res. **10**, 97–209
2 Wright, D. and Mayne, R. (1988) J. Ultrastruct. Mol. Struct. Res. **100**, 224–234
3 Ren, Z., Brewton, R. and Mayne, R. (1991) J. Struct. Biol. **106**, 57–63
4 Wallace, R., Streeten, B. and Hanna, R. (1991) Curr. Eye Res. **10**, 99–109
5 Ross, R., Fialkow, P. and Altman, L. (1976) Adv. Exp. Med. Biol. **79**, 7–15
6 Mecham, R. and Davis, E. (1994) in Extracellular Matrix Assembly and Structure (Yurchenco, P., Birk, D. and Mecham, R., eds.), pp. 281–314, Academic Press, San Diego
7 McGrath, J., Sakai, L. and Eady, R. (1994) Br. J. Dermatol. **131**, 465–471
8 Thurmond, F. and Trotter, J. (1996) J. Exp. Biol. **199**, 1817–1828
9 McConnell, C. J., DeMont, M. E. and Wright, G. M. (1997) J. Physiol. (London) **499**, 513–526
10 Sakai, L., Keene, D. and Engvall, E. (1986) J. Cell Biol. **103**, 2499–2509
11 Sakai, L., Keene, D., Glanville, R. and Baechinger, H. P. (1991) J. Biol. Chem. **266**, 14763–14770
12 Zhang, H., Apfelroth, S., Hu, W., Davis, E., Sanguineti, C., Bonadio, J., Mecham, R. and Ramirez, F. (1994) J. Cell Biol. **124**, 855–863
13 Lee, B., Godfrey, M., Vitale, E., Hori, H., Mattie, M.-G., Sarfarazi, M., Tsipouras, P., Ramirez, F. and Hollister, D. (1991) Nature (London) **352**, 330–334
14 Dietz, H., Cutting, G., Pyeritz, R., Maslen, C., Sakai, L., Corson, G., Puffenberger, E., Hamosh, A., Nanthakumar, E., Curristin, S. et al. (1991) Nature (London) **352**, 337–339
15 Tsipouras, P., Del Mastro, R., Sarfarazi, M., Lee, B., Vitale, E., Child, A., Godfrey, M., Devereux, R., Hewett, D., Steinmann, B. et al. (1992) New Engl. J. Med. **326**, 905–909
16 Corson, G., Chalberg, S., Dietz, H., Charbonneau, N. and Sakai, L. (1993) Genomics **17**, 476–484
17 Pereira, L., D'Alessio, M., Ramirez, F., Lynch, J., Sykes, B., Pangilinan, T. and Bonadio, J. (1993) Hum. Mol. Genet. **2**, 961–968
18 Kanzaki, T., Olofsson, A., Morén, A., Wernstedt, C., Hellman, U., Miyazono, K., Claesson-Welsh, L. and Heldin, C.-H. (1990) Cell **61**, 1051–1061
19 Kielty, C. and Shuttleworth, C. A. (1993) J. Cell Sci. **106**, 167–173
20 Sakai, L. and Keene, D. (1994) Methods Enzymol. **245**, 29–52
21 Sakai, L. (1990) in Elastin: Chemical and Biological Aspects (Tamburro, A. and Davidson, J., eds.), pp. 213–227, Congedo Editore, Galatina, Italy
22 Ross, R. and Bornstein, P. (1969) J. Cell Biol. **40**, 366–381
23 Reinhardt, D., Keene, D., Corson, G., Poeschl, E., Baechinger, H., Gambee, J. and Sakai, L. (1996) J. Mol. Biol. **258**, 104–116
24 Del Sal, G., Manfioletti, G. and Schneider, C. (1989) Biotechniques **7**, 514–519

25 Zhang, H., Hu, W. and Ramirez, F. (1995) J. Cell Biol. **129**, 1165–1176
26 Sambrook, J., Fritsch, E. F. and Maniatis, T. (1989) Molecular Cloning: A Laboratory Manual, 2nd edn., Cold Spring Harbor Laboratory, Cold Spring Harbor, NY
27 Ritty, T. M., Milewicz, D. M. and Mecham, R. P. (1999) J. Biol. Chem. **274**, 8933–8940
28 Milewicz, D. M., Grossfield, J., Cao, S.-N., Kielty, C., Covitz, W. and Jewett, T. (1995) J. Clin. Invest. **95**, 2373–2378
29 Ausubel, F., Brent, R., Kingston, R., Moore, D., Seidman, J., Smith, J. and Struhl, K. (1992) in Current Protocols in Molecular Biology (Kingston, R. E., Kaufman, R. J., Bebbington, C.R and Rolfe, M. R., eds.), pp. 16.14.1–16.14.13, John Wiley, New York
30 Crouch, E., Chang, D., Rust, K., Persson, A. and Heuser, J. (1994) J. Biol. Chem. **269**, 15808–15813
31 Harlow, E. and Lane, D. (1988) Antibodies, A Laboratory Manual, Cold Spring Harbor Laboratory, Cold Spring Harbor, NY
32 Saharinen, J., Taipale, J., Monni, O. and Keski-Oja, J. (1998) J. Biol. Chem. **273**, 18459–18469
33 Qian, R.-Q. and Glanville, R. (1997) Biochemistry **36**, 15841–15847
34 Downing, A. K., Knott, V., Werner, J. M., Cardy, C. M., Campbell, I. D. and Handford, P. A. (1996) Cell **85**, 597–605
35 Kammerer, R. A., Schulthess, T., Landwehr, R., Lustig, A., Fischer, D. and Engel, J. (1998) J. Biol. Chem. **273**, 10602–10608

Received 27 November 1998/22 February 1999; accepted 30 March 1999